Follow the Force: Haptic Communication Enhances Coordination in Physical Human-Robot Interaction When Humans are Followers

Yiming Liu, Raz Leib, and David W. Franklin

***Abstract*—To enhance the integration of robots into daily human life and industrial settings, there is a growing focus on the development of robots capable of physical collaboration with humans. Studies have shown that haptic feedback serves as an essential channel of communication that allows humans to better collaborate with each other. In this study, we investigated the role of haptic communication in physical Human-Robot Interaction (pHRI) tasks, especially in the leader-follower role distribution. We have shown that participants adopted different roles when working with different agents. Haptic feedback promotes a more balanced role distribution between leaders and followers. Moreover, haptic feedback only improved coordination between humans and artificial agents when humans acted as followers. Our findings can potentially enhance robots' ability to anticipate human adaptation and improve their understanding of humans through haptic communication.**

***Index Terms*—Physical human-robot interaction, modeling and simulating humans, human-centered robotics.**

I. Introduction

IN COLLABORATIVE tasks between humans and robots, robots provide many benefits that allow us to achieve better task performance. When collaborating, robots can handle physically demanding and dangerous tasks, while humans can focus on dexterous and decision-making responsibilities. However, such collaborations are more scarce in delicate tasks such as surgical procedures. To have robots cooperate with humans in tasks requiring fine movements or delicate object manipulation, we need transparent collaboration with a high level of mutual understanding between the two sides.

To achieve such transparent collaboration [1], [2], previous studies focused on intent detection [3], [4], [5], role arbitration [6], [7], [8], communication [9], [10] and personalized strategies [11], [12]. While most studies have predominantly concentrated on robot-to-human adaptation, limited literature explores the complementary aspect of adaptation: human-to-robot adaptation [13]. The lack of understanding of how humans adapt to different robot behaviors hinders robots from predicting human actions, which restricts transparent collaboration between humans and robots.

Transparent collaboration relies on the quality and reliability of sensory information shared by both parties. Agents can effectively coordinate their actions through a combination of explicit communication, such as verbal communication, and implicit communication, such as haptic communication [14]. Over the past two decades, studies on human-human collaboration have demonstrated that haptic communication is a rich and nuanced form of communication that facilitates physical collaboration [2], [6], [15], [16], [17]. Furthermore, through haptic communication, humans often develop into different roles during collaboration, such as active leaders and passive followers [13], [18], [19], [20]. However, some key knowledge about the mechanism by which humans utilize haptic communication remains unclear, which limits the application of these findings in the field of pHRI. First, the majority of studies explored simple tasks such as tracking a moving cursor [15], [16], [17] or reaching for a target [19], raising questions about the applicability of these findings to more complex object manipulation tasks that demand greater coordination. Second, the studies can typically only observe the overall impact of haptic communication on the two agents involved. Due to the mutual adaptation between both agents, quantifying the specific changes experienced by each agent becomes challenging. As a result, it remains unclear whether agents in different roles utilize haptic information in similar or distinct ways.

To fill this gap, we designed an experiment where participants needed to collaborate closely with different artificial agents to control a board from both sides and roll the ball on it to the target position. Two different types of artificial agents were employed, with variations in the level of leadership displayed. We aimed to examine how humans adapt to distinct robotic behaviors and how haptic communication impacts coordination when the human participant assumes either a leader or a follower role. Based on previous works on the taxonomy of interactive behaviors [21], we hypothesize that humans will adapt their level of leadership in response to the behavior of the artificial

Manuscript received 15 March 2023; accepted 5 August 2023. Date of publication 21 August 2023; date of current version 29 August 2023. This letter was recommended for publication by Associate Editor M. Sartori and Editor A. Bera upon evaluation of the reviewers' comments. This work was supported in part by Deutsche Forschungsgemeinschaft (DFG, German Research Foundation) under Grant 467042759 and in part by the Imperial-TUM Joint Academy of Doctoral Studies (JADS). The work of Yiming Liu was supported by the TUM International Graduate School of Science and Engineering. *(Corresponding author: David W. Franklin.)*

This work involved human subjects or animals in its research. Approval of all ethical and experimental procedures and protocols was granted by Ethikkommission der TU München under Application No. 763/20 S-KH, and performed in line with the Declaration of Helsinki.

Yiming Liu and Raz Leib are with the Neuromuscular Diagnostics, Department of Sport and Health Sciences, Technical University of Munich, 80992 Munich, Germany (e-mail: yiming.liu@tum.de; raz.leib@tum.de).

David W. Franklin is with the Neuromuscular Diagnostics, Department of Sport and Health Sciences, Technical University of Munich, 80992 Munich, Germany, also with the Munich Institute of Robotics and Machine Intelligence (MIRMI), Technical University of Munich, 80992 Munich, Germany, and also with the Munich Data Science Institute (MDSI), Technical University of Munich, 80992 Munich, Germany (e-mail: david.franklin@tum.de).

This letter has supplementary downloadable material available at https://doi.org/10.1109/LRA.2023.3307006, provided by the authors.

Digital Object Identifier 10.1109/LRA.2023.3307006

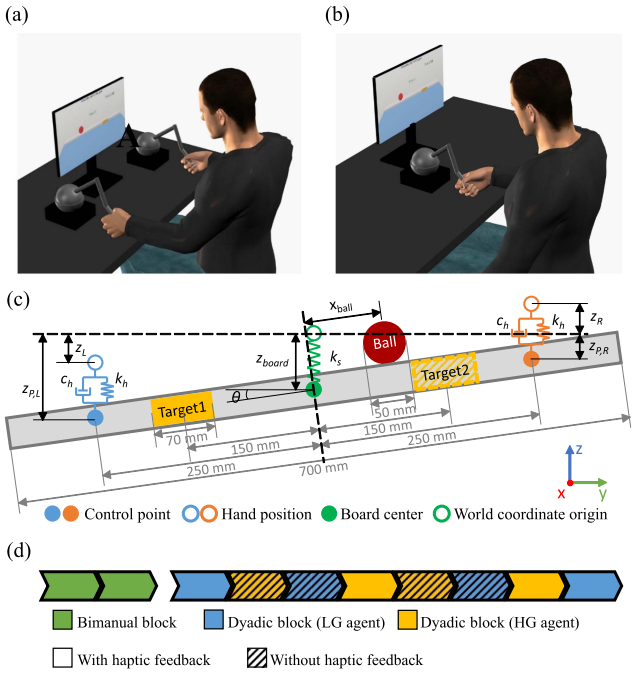

Fig. 1. Experimental setup. (a) The bimanual experimental setup. (b) The dyadic experimental setup. The participant in the dyadic blocks only controlled the left side of the board, while an artificial agent controlled the right side. (c) The dynamics of the virtual experiment model. Participants controlled the board via a spring-damper system, and the center of the board was attached to the origin of the world coordinate by a spring. (d) An example of the experiment protocol. The order of the dyadic blocks was randomized for each participant.

agent. This adaptation aims to optimize the trade-off between minimizing errors and minimizing effort. Additionally, we propose that leaders and followers demonstrate distinctive patterns in their utilization of haptic communication.

II. Materials and Methods

A. Participants

Eleven right-handed participants (19–39 years of age, seven females, handedness assessed using the Edinburgh Inventory [22]) participated in the study after providing written informed consent. All participants were neurologically healthy and were naive to the purpose of the study. The study was approved by the institutional ethics committee at TUM. Before the experiment, participants were introduced to and familiarized with the haptic devices. Five participants had used these devices in previous experiments.

B. Experimental Apparatus

Participants sat in front of a screen and grasped the handles of robotic haptic devices (Phantom Touch, 3D SYSTEMS). The task was to control the rotation and vertical position of a board to slide a ball into a target area. In the bimanual condition, participants held one robotic device in each hand and used both hands to control the two sides of the board (Fig. 1(a)). In the dyadic condition, participants only held one haptic device with their dominant hand and only controlled the left side of the board (Fig. 1(b)). The right side was controlled by an artificial agent. The experiment was conducted in a virtual reality environment rendered by Chai3D [23].

The dimensions of each part of the board-ball model are marked in Fig. 1(c). The center of the board was not spatially fixed in the virtual environment but connected to the origin of the environment by a virtual spring. This spring generated force feedback according to the deviation of the center of the board. This provided participants with haptic information regarding the partner's position. The spring's stiffness was configured to enable unrestricted movement for both sides without being constricted by the partner. The positive directions of the x, y, and z coordinates are perpendicular to the screen to the outside, to the right, and to the top, respectively (Fig. 1(c)). The agents manipulated the z-coordinates of the control points of the board by exerting forces through spring-damper mechanisms. The hand movement was restricted by the program to the vertical direction. The board's movement was limited to translation along the z-axis and rotation around the x-axis. The ball could only move along the long side of the board. The target area can be in one of two possible positions, switching between them for each trial.

C. Design of the Artificial Agent

The goal of this experiment was to examine the role adaptation of humans to artificial agents during an object manipulation task. For this reason, the artificial agent side was designed as a non-adaptive PD controller. The position of the artificial agent was controlled as follows:

$$\hat{z}_R = k_{bp}\left(x_{ball} - x_t\right) + k_{bv}\,\dot{x}_{ball} \tag{1}$$

$$\dot{z}_R = k_v\left(\hat{z}_R - z_R\right) \tag{2}$$

where $\hat{z}_{\mathrm{R}}$ is the desired position of the artificial agent and z_{R} is the actual position. x_{ball} and x_{t} are the relative positions of the ball and the center of the target area along the long side of the board. $k_{\mathrm{v}} = 5$ was empirically selected to ensure that the velocity of the artificial agents and the participants were within a similar range.

We designed two types of artificial agents: the high-gain (HG) and the low-gain (LG) agent. For the HG agent, $k_{\mathrm{bp}} = k_{\mathrm{bv}} = 0.18$. For the LG agent, $k_{\mathrm{bp}} = k_{\mathrm{bv}} = 0.03$. The values were selected based on our previous experiment [24], such that the HG agent is more active and the LG agent is more passive than most participants. Since participants required time to react after the start of each trial, the artificial agent remained stationary for 0.6 seconds at the start of a trial.

D. Experimental Paradigm

Each trial started with the ball fixed at the center of one target area. Participants were given auditory and visual cues to start controlling the board, aiming to move the ball and stabilize it in the opposite target area. The trial was completed when the ball remained in the target area for 1.5 seconds. Participants were then required to keep the board horizontal until the next trial started. At this point, the target area switched to the opposite side to start the next trial. If the ball fell off the edge of the board, the trial would be marked as failed and was repeated. Participants could see the completion time after each trial and were encouraged to complete the trials as fast as possible.

Each participant performed ten experimental blocks. Each block consisted of 60 successful trials with the same experimental condition. The first two blocks included bimanual manipulation with haptic feedback that served to familiarize the

TABLE I
PARAMETERS OF THE VIRTUAL BOARD-BALL MODEL

Symbol	Parameter	Unit	Value
M	Weight of the board	kg	0.01
m	Weight of the ball	kg	0.05
g	Gravity acceleration	m/s^2	9.81
k_h	Force input stiffness	N/m	200
c_h	Force input damper	Ns/m	2
k_s	Stiffness of the spring	N/m	140
l	Distance between the control point and the center of the board	m	0.25
I	Moment of inertia of the board	$kg \cdot m^2$	0.0004

participants with the task. The remaining eight blocks were all dyadic experiments, with participants controlling the left side and the artificial agent controlling the right side of the board. In each block, we implemented one type of artificial agent (HG or LG) and either provided or blocked haptic feedback totaling to four different block types. For the blocks with haptic feedback, the participant could feel the force through the haptic device. The haptic device generated no forces in blocks without haptic feedback.

Each block type appeared twice, totaling to eight blocks. The blocks appeared in two rounds in which we randomized their appearance between participants. Before each block started, participants were unaware of the condition. An example experimental protocol is depicted in Fig. 1(d).

E. Virtual Board-Ball Model

By moving their hands, participants generated forces on the board at the two control points. The forces were generated according to (3).

$$F_{side} = k_h \cdot (z_{side} - z_{P,side}) + c_h \cdot (\dot{z}_{side} - \dot{z}_{P,side}) \quad (3)$$

where $side = \{L, R\}$, referring to the left (human) or right (artificial agent) side. F_{side} is the generated force, z_{side} and $z_{\text{P,side}}$ are the z coordinates of the hand and the control point, respectively. The motion of the board and the ball were simulated as follows:

$$F_s = -k_s \, z_{board} \quad (4)$$

$$F_L + F_R - M\,g - m\,g\,\cos^2\theta + F_s = M\,\ddot{z}_{board} \quad (5)$$

$$(F_R - F_L)\,l\,\cos\theta - m\,g\,x_{ball}\cos\theta = I\,\ddot{\theta} \quad (6)$$

$$m\,\ddot{x}_{ball} = m\,g\,\sin\theta \quad (7)$$

In these equations, F_{s} is the force generated by the spring connected to the center of the board. z_{board} is the z coordinate of the center of the board. θ is the board's angle around the x-axis with positive values marking counterclockwise rotation. The values and meanings of the other parameters are summarized in Table I.

F. Data Analysis

Kinematic and dynamic data were sampled at 1000 Hz and low-pass filtered with a tenth-order, zero-phase-lag Butterworth filter with a 20 Hz cutoff frequency to remove any high-frequency noise. P values less than 0.05 were considered statistically significant and were denoted with *($p < 0.05$), **($p < 0.01$), ***($p < 0.001$) and ****($p < 0.0001$).

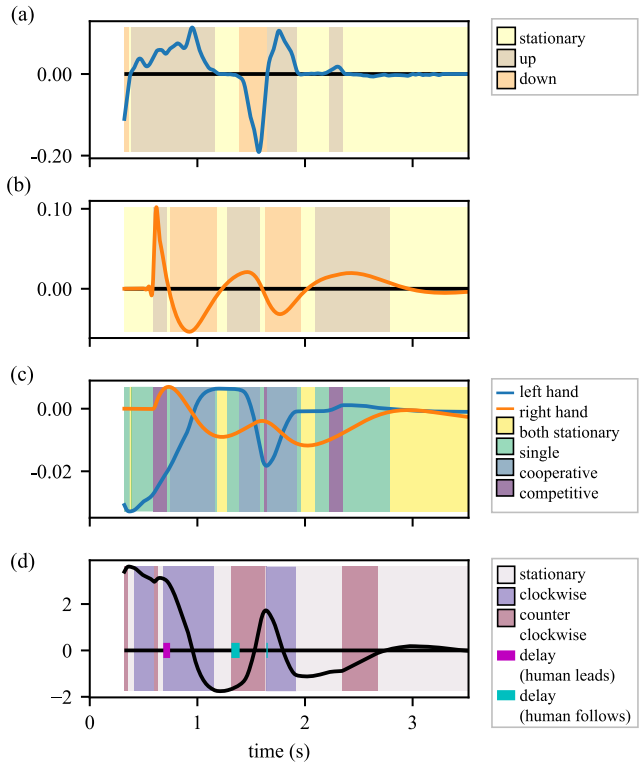

Fig. 2. Example of a representative trial. (a, b) Velocity profile and HMM hand movement segmentation for the left and right sides, respectively. (c) Left and right hand trajectories and the collaboration dynamics. (d) Angle of the board, the HMM board rotation segmentation, and the extracted delay between the agents.

1) Completion Time: Completion time was defined as the time from the beginning of each trial to when the ball stayed in the target area for 1.5 s.

2) Movement Segmentation: We observed that participants generally controlled the board with a series of discrete movements rather than continuous ones. To identify the start and end of the movements in each trial, we performed unsupervised segmentation of the velocity profile of the hand and the board using a hidden Markov Model (HMM) [25]. For hand movement segmentation, we trained an HMM for each participant using the hand velocity profiles of the agents of all trials. The HMM classified the hand movement into one of three states: moving down, stationary, or moving up (Fig. 2(a)). Similarly, we trained an HMM for the rotational motion of the board. This HMM used the angular velocity profile of the board to predict if it is rotating clockwise, stationary, or rotating counterclockwise (Fig. 2(c)).

3) Coordination: Coordination refers to the ability to work together effectively and efficiently to achieve a common goal. In this study, coordination means that the two agents are synchronized and try to rotate the board in the same direction. We quantify the coordination by collaboration dynamics and by delay.

a) Collaboration dynamics: Based on the results of hand movement segmentation, each side could only be in one of three states at each time point: Moving up, moving down, or stationary. Consequently, there were nine possible combinations of movement states between the two sides. To label the collaboration dynamics, we grouped these nine combinations into four categories:

- Cooperative movement: the two sides were moving in opposite directions.
- Competitive movement: both sides were moving in the same direction.
- Single movement: one side was moving while the other side was not.
- Stationary: both sides were not moving.

An example of collaboration dynamics is depicted in Fig. 2(b). To determine the proportion of each collaboration category, the total time spent on each category was divided by the completion time of the trial.

b) Delay: When both sides try to rotate the board in the same direction, it is common for one side to start first and the other side to follow. This time difference was defined as the delay. Based on the results of the movement segmentation, we calculated the delay between the participant and the artificial agent for each board movement segment. If there is a cooperative movement within a board movement segment, the time from the start of this board movement segment to the start of the cooperative movement is the delay of this segment (see Fig. 2(c)). The delay is positive when the artificial agent moves ahead of the human and negative otherwise. Board movement segments without cooperative movement were discarded from this analysis. The delay during the first 0.6 seconds of each trial was not considered since the artificial agent was programmed to remain still (see *Design of the Artificial Agent*). We calculated each trial's mean absolute delay of all the board segments. We defined the following delay as the mean of all delays when humans followed the artificial agent and the leading delay as the mean of all delays when humans were leading.

4) Strategy and Leader-Follower Relationship: We used linear models to quantify the individual strategy and contribution of the participants and the artificial agent. In this study, the manipulation task was shared by the two agents. The more active and contributing agent was defined as the leader, while the other was the follower. These roles were determined based on the extracted control gains as follows.

a) Ball-Hand Model: We modeled the participants as controlling the position and velocity of the ball in a linear model, similar to a PD controller. We defined a linear model that mapped the position and velocity of the ball to hand positions to quantify the individual strategies.

$$z_L = -k_{bpos-L} * (x_{ball} - x_t) - k_{bvel-L} * \dot{x}_{ball} + b_{b-L} \quad (8)$$

$$z_R = k_{bpos-R} * (x_{ball} - x_t) + k_{bvel-R} * \dot{x}_{ball} + b_{b-R} \quad (9)$$

where $k_{\text{bpos-L}}$, $k_{\text{bpos-R}}$, $k_{\text{bvel-L}}$, $k_{\text{bvel-R}}$, $b_{\text{b-L}}$ and $b_{\text{b-R}}$ are the ball position gain, ball velocity gain and intersection of the human and artificial agent, respectively (Fig. 3(a)). Higher gains in ball position and velocity indicate a more active strategy by the agent.

b) Angle-Hand Model: Similarly, we used a second linear model to map the board angles to hand positions. This model shows the amount of movement on each side when the board was rotated to a specific angle.

$$z_L = -k_{\theta-L} * \theta + b_{\theta-L} \quad (10)$$

$$z_R = k_{\theta-R} * \theta + b_{\theta-R} \quad (11)$$

where $k_{\theta\text{-L}}$, $k_{\theta\text{-R}}$, $b_{\theta\text{-L}}$ and $b_{\theta\text{-R}}$ are the gains and intersection points of the human and artificial agent, respectively (Fig. 3(b)). Due to physical limitations, the total movement of the left and right sides in opposite directions is fixed when the board is rotated to a specific angle without translation. Therefore, $k_{\theta\text{-L}}$ and $k_{\theta\text{-R}}$ should sum to a constant value, and their ratio indicates the relative contribution of the two agents in controlling the board's motion.

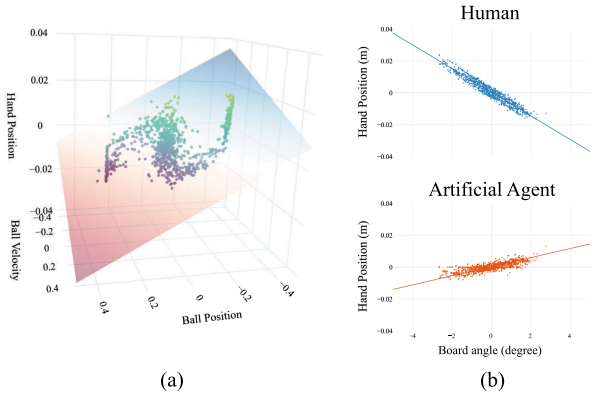

Fig. 3. Linear models of a typical participant. (a) The ball-hand model. The scatter points are the ball position, ball velocity, and hand position at the end of each board movement segment. These scatter points are approximately located on the semi-transparent plane representing the linear model. (b) The angle-hand model. The scatter points are the board angle and hand position at the end of each board movement segment. The scatter points lie approximately on a line representing the linear model. The upper and lower panels depict the human and the artificial agent, respectively. The human is the leader of this block, as indicated by the higher gain (i.e., the larger slope of the line) compared to the artificial agent.

$$p_{\theta-L} = k_{\theta-L}/(k_{\theta-L} + k_{\theta-R}) \quad (12)$$

$$p_{\theta-R} = k_{\theta-R}/(k_{\theta-L} + k_{\theta-R}) \quad (13)$$

where $p_{\theta\text{-L}}$, $p_{\theta\text{-R}}$ are the proportions of the angle-hand gain. The agents with a higher proportion have a more dominant role than their partners. Thus they are defined as the leaders, while their partners are defined as the followers.

Comparing the movement of the human and the artificial agent (Fig. 2(a) and (b)), we see that humans often produced discrete movements [26], while the artificial agent generated continuous movements. Therefore, we propose that the hand positions at every time step do not indicate the participants' desired position. Instead, we assume that the participants arrived at their desired position at the end of each board movement segment. We took the θ, x_{ball}, $\dot{x}_{\text{ball}}$, z_{L}, z_{R} at the end of each board movement segment and used linear regression algorithm to fit the parameters.

III. Results

A. Learning Effect

As participants were instructed to complete the task as quickly as possible, completion time is an intuitive metric for quantifying performance. Participants' completion time improved during the first two bimanual familiarization blocks (Fig. 4(a)). In the subsequent dyadic blocks, the completion time showed higher values at the beginning of each block, then quickly decreased and reached a stable level as participants adapted to the specific conditions and exhibited a consistent level of performance. Differences in completion time across the four conditions in dyadic blocks are shown in Fig. 4(b). A repeated measures two-way ANOVA indicated that the interaction between the gain of the artificial agent (LG or HG) and haptic feedback (with or without) factors was significant ($F(1, 10) = 8.97$, $p = 0.013$). Post-hoc

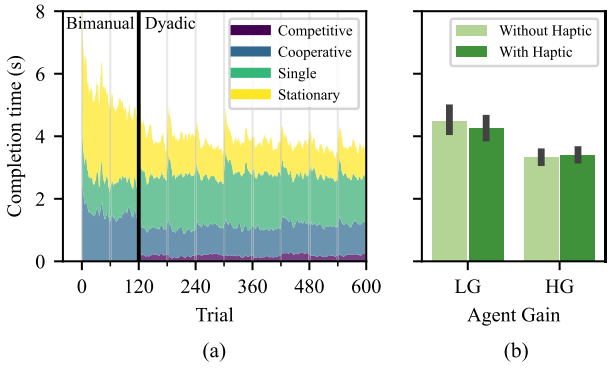

Fig. 4. Completion time. (a) All participants' average completion time and proportion of each state of collaboration dynamics. The data for the 600 trials of 10 blocks is presented in the order in which each individual completed them. The first 120 familiarization trials were bimanual, while the remaining trials were dyadic. Note, that the conditions experienced by each participant during a given dyadic block may vary and were averaged together. (b) The average completion time and 95% confidence intervals of the four conditions.

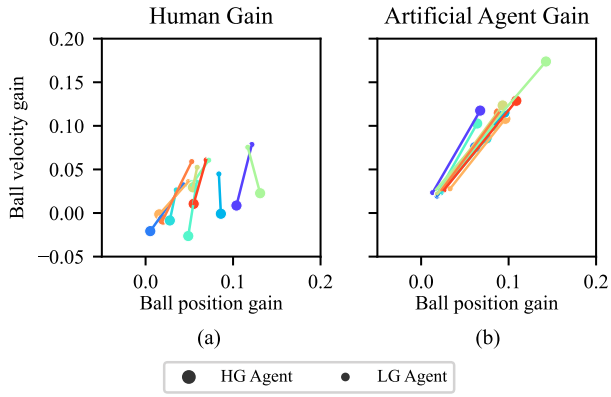

Fig. 5. Ball position and velocity gains. (a) Human participants. (b) Artificial agents. Participants are color-coded, and conditions involving LG and HG agents are denoted by smaller and larger dots, respectively. The closer the data points are to the top right of the figure, the more active the participants are.

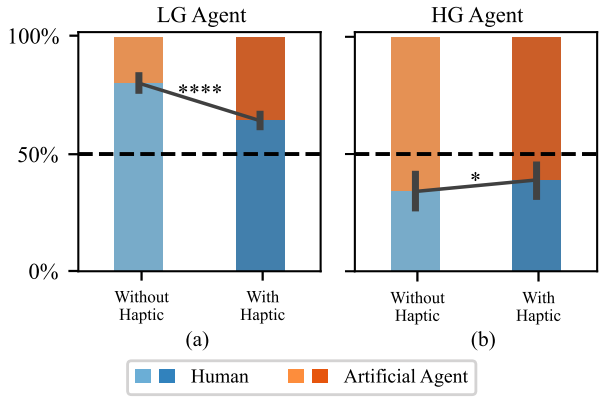

Fig. 6. Average and 95% confidence interval of the proportion of angle-hand gain in different artificial agent gain and haptic conditions. (a) LG Agent. (b) HG Agent.

paired t-tests with Bonferroni correction revealed that haptic feedback did not have a significant impact on the completion time (LG agent ($t(10) = -2.40$, $p = 0.074$), HG agent ($t(10) = 1.10$, $p = 0.060$)). When paired with the same artificial agent, participants completed the task in a similar amount of time regardless of whether haptic feedback was provided.

The proportion of each category of collaboration dynamics was color-coded in Fig. 4(a). In dyadic blocks, there was an evident increase in the proportion of competitive and single movements, while the proportion of cooperative and stationary behavior decreased compared to bimanual blocks. This is to be expected, as it is more challenging to coordinate with the partner than with one's own two hands.

B. Leader-Follower Role Distribution

This subsection investigates the adjustment of role distribution between participants and artificial agents and the influence of haptic communication on this process. Since the HG agent was designed to be much more proactive than the LG agent, participants were expected to adapt their strategies and switch between leader and follower roles based on the behavior of the artificial agent.

The role distribution was initially assessed by ball position gain and ball velocity gain (Fig. 5). Points closer to the upper right corner represent higher gains, which indicate more active strategies, while points near the lower left corner reflect more passive strategies. All participants switched to a more active strategy with the LG agent and assumed the leader role. Conversely, they adopted a more passive strategy with the HG agent, taking on the follower role.

The role distribution was then assessed by the proportion of the angle-hand gain $p_{\theta\text{-L}}$ and $p_{\theta\text{-R}}$ (Fig. 6). The proportion of participants' contribution varied with the agent they interacted with, being more than 50% with the LG agent and less than 50% with the HG agent. This again confirms their expected role adaptation as leaders and followers. This adaptation of role distribution was simulated by an LQG controller, as demonstrated in Section IV.

Moreover, we observed that haptic feedback influenced the role distribution. A repeated measures two-way ANOVA on $p_{\theta\text{-L}}$ indicated that the interaction between the gain of the artificial agent and haptic feedback factors was significant ($F(1, 10) = 170.20$, $p < 0.0001$). Further post-hoc paired t-tests with Bonferroni correction showed that haptic feedback led to a significant reduction in human's proportion with the LG agent ($t(10) = -14.12$, $p < 0.0001$), and a significant increase with the HG agent ($t(10) = 2.79$, $p = 0.038$). In both cases, the proportion shifted towards 50% when haptic feedback was available (Fig. 6), indicating decreased dominance in leaders and increased activity in followers. We concluded that the integration of haptic feedback results in a more balanced distribution of responsibilities within the leader-follower dynamic. In other words, the leader-follower relationship is reinforced in the absence of haptic feedback.

C. Coordination Between the Two Agents

Until now, our investigation has primarily focused on analyzing trial-level data, treating each trial as a whole. In this section, we delved into the time series data, exploring the influence of haptic communication on the coordination between the

two agents. We hypothesized that haptic communication might increase the level of coordination. We quantified coordination by collaboration dynamics and delay.

As defined in Section II, collaboration dynamics were categorized into four types: cooperative, competitive, single, and stationary. We examined the change in the proportion of each category of collaboration dynamics when working with the LG or HG agent with or without haptic feedback (Fig. 7(a) and (b)). We conducted a repeated measures two-way ANOVA on each of the four categories. The interaction between the gain of the artificial agent and haptic feedback factors was significant for cooperative movement ($F(1, 10) = 28.025$, $p = 0.0003$) and single movement ($F(1, 10) = 9.98$, $p = 0.010$), but not significant for stationary ($F(1, 10) = 2.737$, $p = 0.129$) or competitive movement ($F(1, 10) = 1.11$, $p = 0.318$). Further post-hoc paired t-tests with Bonferroni correction showed that, for the HG agent, haptic feedback led to a significant increase in cooperative movement proportion ($t(10) = 6.69$, $p = 0.0001$) and a significant decrease in single movement proportion ($t(10) = -3.669$, $p = 0.009$). This indicated improved coordination between the participant and the HG agent due to haptic feedback. The same trend was found when comparing dyadic with bimanual blocks (Fig. 4), as the coordination between one's two hands is expected to be better than between two agents. However, haptic feedback showed no statistically significant impact for the LG agent (cooperative ($t(10) = -1.68$, $p = 0.249$), single ($t(10) = 0.057$, $p = 1.0$)).

Similarly, haptic feedback also influenced the delay between the two agents (Fig. 7(c) and (d)). We conducted repeated-measures two-way ANOVAs on the absolute delay, following delay, and leading delay. The interaction between the gain of the artificial agent and haptic feedback factors was significant for absolute delay ($F(1,10) = 8.46$, $p = 0.016$) and following delay ($F(1,10) = 7.09$, $p = 0.024$) but not for leading delay ($F(1,10) = 0.75$, $p = 0.408$). Post-hoc paired t-tests with Bonferroni correction showed that, with the HG agent, absolute delay ($t(10) = -3.00$, $p = 0.013$) and following delay ($t(10) = -2.71$, $p = 0.022$) both decreased significantly. No significant change was observed with the LG agent (absolute delay ($t(10) = -0.87$, $p = 0.407$), following delay ($t(10) = -1.96$, $p = 0.079$)). This again shows that delay, especially when humans followed artificial agents, only decreased with the HG agent but not with the LG agent.

In Fig. 7(e) and (f), we illustrated the change in coordination due to haptic feedback by the two most representative factors: the proportion of cooperative movement and absolute delay. With the LG agent (Fig. 7(e)), participants exhibited small changes in different directions. However, most participants shifted to the bottom right corner with the HG agent (Fig. 7(f)), which shows improved coordination due to haptic feedback. The results from collaboration dynamics and delay were consistent: Haptic feedback improved coordination only when humans acted as followers with the HG agent, but not when humans acted as leaders with the LG agent.

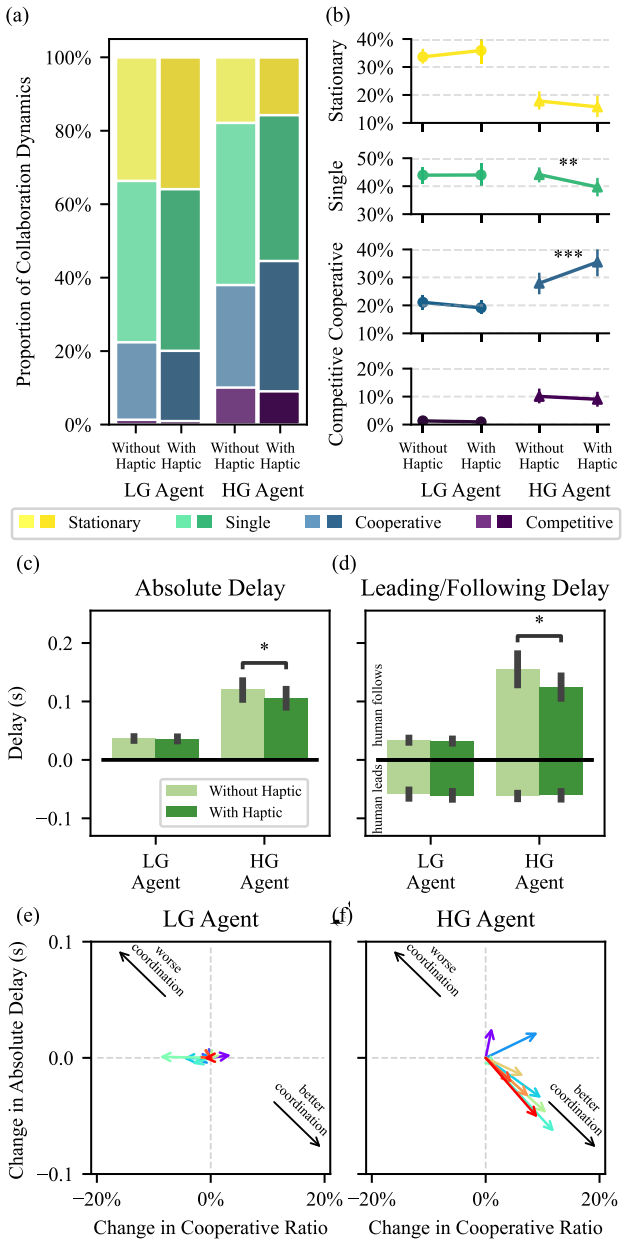

Fig. 7. Coordination between the two agents. (a) The proportion of each category of collaboration dynamics. (b) The average and 95% confidence interval of the proportion of each category. (c) The mean absolute delay. (d) The upper part displays the following delay when the human follows the artificial agent, while the lower part shows the leading delay when the human leads the artificial agent. (e) Change in coordination due to haptic feedback during interaction with the LG agent. The arrows indicate the change in the proportion of cooperative movement (x-axis) and absolute delay (y-axis) for each participant (color-coded). Arrows pointing to the lower right indicate improved coordination with haptic feedback, while those pointing to the upper left show decreased coordination. (f) Interaction with the HG agent.

IV. Modeling the Role Distribution Using LQG

Optimal feedback control models can well explain a broad range of human movements [27]. In recent years, this framework has been used to explain physical collaboration between multiple agents [21], [28]. Jarrassé et al. [21] explained the role distribution in shared control as a trade-off between minimizing error and minimizing effort. They simulated different types of role distribution by adjusting the cost function. Based on this idea, we designed an LQG controller to control the board on the left side, with the same LG and HG agents on the right side. By incorporating the dynamics of the artificial agent in the state space equation of the LQG, we observed that the controller adapted to the leader role with the LG agent and the follower role with the HG agent, similar to human behavior. This was

achieved without any modifications to the cost function. We used a linearized representation of the system (14).

$$\dot{x} = Ax + Bu$$

$$x' = \begin{bmatrix} x_{ball} & \dot{x}_{ball} & \theta & \dot{\theta} & \tilde{z}_{board} & \dot{\tilde{z}}_{board} & z_L & z_R \end{bmatrix}$$

$$A' = \begin{bmatrix} 0 & 0 & 0 & \frac{5c_h l k_r - mg}{I} & 0 & \frac{5k_r c_h}{M} & 0 & 5k_r \\ 1 & 0 & 0 & \frac{5c_h l k_r}{I} & 0 & \frac{5k_r c_h}{M} & 0 & 5k_r \\ 0 & -g & 0 & \frac{-2l^2 k_h}{I} & 0 & 0 & 0 & 0 \\ 0 & 0 & 1 & \frac{-2l^2 c_h}{I} & 0 & 0 & 0 & 0 \\ 0 & 0 & 0 & 0 & 0 & \frac{-2k_h - k_{spring}}{M} & 0 & 0 \\ 0 & 0 & 0 & 0 & 1 & \frac{-2c_h}{M} & 0 & 0 \\ 0 & 0 & 0 & \frac{-k_h l + 5c_h l}{I} & 0 & \frac{k_h - 5c_h}{M} & -5 & 0 \\ 0 & 0 & 0 & \frac{k_h l - 5c_h l}{I} & 0 & \frac{k_h - 5c_h}{M} & 0 & -5 \end{bmatrix}$$

$$B' = \begin{bmatrix} 0 & 0 & 0 & -\frac{5lc_h}{I} & 0 & \frac{5c_h}{M} & 5 & 0 \end{bmatrix}$$

$$\tilde{z}_{board} = z_{board} - \frac{(m+M)g}{k_{spring}} \tag{14}$$

where u is the control output generated by the LQG controller and $\tilde{z}_{\text{board}}$ is the modified z coordinate of the board in order to linearize the system. The state-cost weighted matrix (Q) and input-cost weighted matrix (R) are:

$$Q = \boldsymbol{diag}\{100, 100, 1, 1, 1, 1, 1, 1\},\ R = 7000$$

We added Gaussian noise to the measured states and used a Kalman filter as a state observer to estimate the actual state values using the noisy signals. We simulated the task with the LQG controller for 30 trials for each of the LG and HG agents. The average trajectory shows that the LQG controller exhibited more active movements in a broader range when partnered with the LG agent compared with the HG agent (Fig. 8(a) and (b)). This was consistent with human participants (see Fig. 8(c) and (d) as a reference). We further calculated the ball position and velocity gain (Fig. 8(e)) and the proportion of angle-hand gain (Fig. 8(f)). We saw a clear shift in roles in both plots. In conclusion, the LQG controller took on different leader/follower roles for different artificial agents in a human-like way. This suggests that humans may adjust role distribution in an optimal control manner.

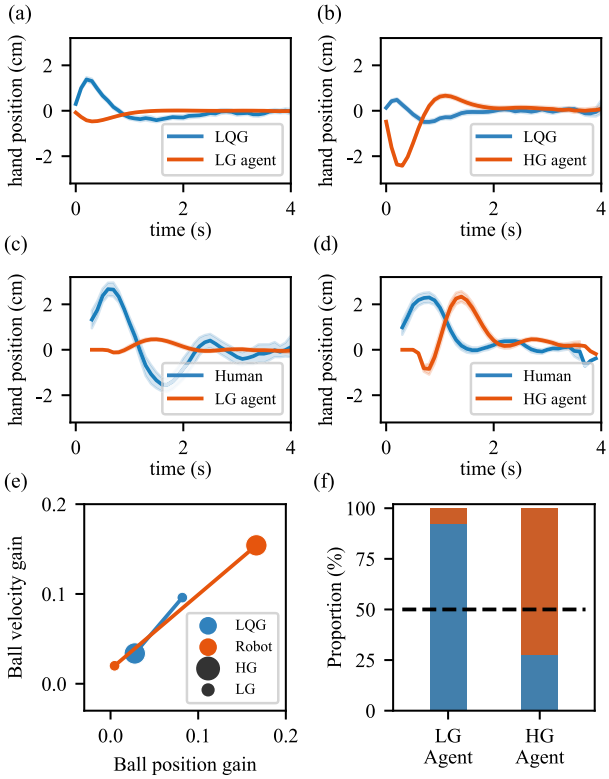

Fig. 8. Simulating human behavior with an LQG controller. (a–b) The average trajectory of 30 trials of the left and right sides. The left side was controlled by the LQG controller, and the right side was controlled by the LG/HG agent. The shaded area represents the 95% confidence interval. (c–d) For comparison, the average trajectory of 30 trials, where participant p1 controlled the left side and the LG/HG agent controlled the right side. (e) the ball position gain and ball velocity gain of the LQG simulation. (f) The proportion of angle-hand gain of the LQG simulation.

V. Discussion

In this study, we investigated a more complex task of manipulating objects with internal degrees of freedom, which is a further exploration toward understanding shared control. The results of our study suggest that individuals tend to adopt leader or follower roles based on the activity level of the artificial agent. In this process, haptic feedback promoted a more balanced distribution of task-related responsibilities between humans and artificial agents, whereas its absence enhanced the leader-follower relationship, aligning with [29]. Furthermore, we successfully disentangled the individual changes of the collaborating agents and found that haptic communication led to improved coordination when humans assumed follower roles. However, no improvement in coordination was observed when humans were leaders.

When participants collaborated with the HG agent, one possible explanation of the observed outcome is that the absence of haptic communication introduced challenges in coordinating with the artificial agent due to the increased difficulty in inferring the artificial agent's intentions [16]. Consequently, participants lowered their level of leadership further, enabling the artificial agent to assume a more dominant role in the task, thereby achieving task completion within a comparable time. This process is similar to the shared autonomy paradigm, where the robot can adapt its level of autonomy based on its understanding of human behavior [30].

The different impact of haptic communication on coordination, with improvements observed only when humans assumed follower roles but not leader roles, suggests that these roles may have different responsibilities and distinct utilization of haptic information. The follower's responsibility may include maintaining coordination, whereas leaders may primarily prioritize task performance.

Our study takes a step towards understanding human-to-robot adaptation, which received less attention compared to robot-to-human adaptation in pHRI. To the best of our knowledge, our study is the first to demonstrate the different effects of haptic communication on leaders and followers. Our findings can potentially enhance robots' ability to anticipate human adaptation to different robot behaviors. Within the context of human-robot collaboration, humans typically assume leader roles while robots act as followers. Our results indicate that haptic feedback may contain information that is not visually

observable, which allows robots to better understand and coordinate with human leaders, thereby enhancing the transparency of the collaboration. However, the mechanism for utilizing this haptic information requires further exploration. The presented task is simplified, so the extent to which our findings can be generalized to more complex real-world tasks remains to be determined.

ACKNOWLEDGMENT

The authors thank Jacqueline Mitzenmacher (MIT, USA) for her assistance in conducting the experiments.

REFERENCES

[1] A. Ajoudani, A. M. Zanchettin, S. Ivaldi, A. Albu-Schäffer, K. Kosuge, and O. Khatib, "Progress and prospects of the human–robot collaboration," *Auton. Robots*, vol. 42, no. 5, pp. 957–975, 2018.

[2] D. P. Losey, C. G. McDonald, E. Battaglia, and M. K. O'Malley, "A review of intent detection, arbitration, and communication aspects of shared control for physical human–robot interaction," *Appl. Mechanics Rev.*, vol. 70, no. 1, 2018, Art. no. 010804.

[3] Z. Wang et al., "Probabilistic movement modeling for intention inference in human–robot interaction," *Int. J. Robot. Res.*, vol. 32, no. 7, pp. 841–858, 2013.

[4] Z. Wang, A. Peer, and M. Buss, "An HMM approach to realistic haptic human-robot interaction," in *Proc. World Haptics 3rd Joint EuroHaptics Conf. Symp. Haptic Interfaces Virtual Environ. Teleoperator Syst.*, 2009, pp. 374–379.

[5] M. S. Erden and T. Tomiyama, "Human-intent detection and physically interactive control of a robot without force sensors," *IEEE Trans. Robot.*, vol. 26, no. 2, pp. 370–382, Apr. 2010.

[6] K. B. Reed and M. A. Peshkin, "Physical collaboration of human-human and human-robot teams," *IEEE Trans. Haptics*, vol. 1, no. 2, pp. 108–120, Jul.–Dec. 2008.

[7] Y. Li, K. P. Tee, W. L. Chan, R. Yan, Y. Chua, and D. K. Limbu, "Continuous role adaptation for human–robot shared control," *IEEE Trans. Robot.*, vol. 31, no. 3, pp. 672–681, Jun. 2015.

[8] R. Ueha, H. T. Pham, H. Hirai, and F. Miyazaki, "A simple control design for human-robot coordination based on the knowledge of dynamical role division," in *Proc. IEEE/RSJ Int. Conf. Intell. Robots Syst.*, 2009, pp. 3051–3056.

[9] S. Li and X. Zhang, "Implicit intention communication in human–robot interaction through visual behavior studies," *IEEE Trans. Human-Mach. Syst.*, vol. 47, no. 4, pp. 437–448, Aug. 2017.

[10] S. Grushko, A. Vysockỳ, P. Oščádal, M. Vocetka, P. Novák, and Z. Bobovskỳ, "Improved mutual understanding for human-robot collaboration: Combining human-aware motion planning with haptic feedback devices for communicating planned trajectory," *Sensors*, vol. 21, no. 11, 2021, Art. no. 3673.

[11] L. Peternel, N. Tsagarakis, D. Caldwell, and A. Ajoudani, "Robot adaptation to human physical fatigue in human–robot co-manipulation," *Auton. Robots*, vol. 42, no. 5, pp. 1011–1021, 2018.

[12] A. Shafti, J. Tjomsland, W. Dudley, and A. A. Faisal, "Real-world human-robot collaborative reinforcement learning," in *Proc. IEEE/RSJ Int. Conf. Intell. Robots Syst.*, 2020, pp. 11161–11166.

[13] L. Vianello, S. Ivaldi, A. Aubry, and L. Peternel, "The effects of role transitions and adaptation in human-cobot collaboration," *J. Intell. Manuf.*, pp. 1–15, 2023.

[14] N. Gildert, A. G. Millard, A. Pomfret, and J. Timmis, "The need for combining implicit and explicit communication in cooperative robotic systems," *Front. Robot. AI*, vol. 5, 2018, Art. no. 65.

[15] A. Takagi, G. Ganesh, T. Yoshioka, M. Kawato, and E. Burdet, "Physically interacting individuals estimate the partner's goal to enhance their movements," *Nature Hum. Behav.*, vol. 1, no. 3, pp. 1–6, 2017.

[16] A. Takagi, F. Usai, G. Ganesh, V. Sanguineti, and E. Burdet, "Haptic communication between humans is tuned by the hard or soft mechanics of interaction," *PLoS Comput. Biol.*, vol. 14, no. 3, 2018, Art. no. e1005971.

[17] A. Takagi, M. Hirashima, D. Nozaki, and E. Burdet, "Individuals physically interacting in a group rapidly coordinate their movement by estimating the collective goal," *Elife*, vol. 8, 2019, Art. no. e41328.

[18] S. Nakayama, M. Ruiz Marín, M. Camacho, and M. Porfiri, "Plasticity in leader–follower roles in human teams," *Sci. Rep.*, vol. 7, no. 1, pp. 1–9, 2017.

[19] A. Takai et al., "Learning acquisition of consistent leader–follower relationships depends on implicit haptic interactions," *Sci. Rep.*, vol. 13, no. 1, 2023, Art. no. 3476.

[20] A. Mörtl, M. Lawitzky, A. Kucukyilmaz, M. Sezgin, C. Basdogan, and S. Hirche, "The role of roles: Physical cooperation between humans and robots," *Int. J. Robot. Res.*, vol. 31, no. 13, pp. 1656–1674, 2012.

[21] N. Jarrassé, T. Charalambous, and E. Burdet, "A framework to describe, analyze and generate interactive motor behaviors," *PLoS One*, vol. 7, no. 11, 2012, Art. no. e49945.

[22] R. C. Oldfield, "The assessment and analysis of handedness: The Edinburgh inventory," *Neuropsychologia*, vol. 9, no. 1, pp. 97–113, 1971.

[23] F. Conti, F. Barbagli, D. Morris, and C. Sewell, "Chai 3D: An open-source library for the rapid development of haptic scenes," *IEEE World Haptics*, vol. 38, no. 1, pp. 21–29, Mar. 2005.

[24] Y. Liu, R. Leib, W. Dudley, A. Shafti, A. A. Faisal, and D. W. Franklin, "The role of haptic communication in dyadic collaborative object manipulation tasks," 2022, *arXiv:2203.01287*.

[25] L. E. Baum and T. Petrie, "Statistical inference for probabilistic functions of finite state Markov chains," *Ann. Math. Statist.*, vol. 37, no. 6, pp. 1554–1563, 1966.

[26] T. Insperger, "Act-and-wait concept for continuous-time control systems with feedback delay," *IEEE Trans. Control Syst. Technol.*, vol. 14, no. 5, pp. 974–977, Sep. 2006.

[27] J. Česonis and D. W. Franklin, "Mixed-horizon optimal feedback control as a model of human movement," *Neurons, Behav., Data Anal. Theory*, vol. 1, pp. 1–36, 2021, doi: 10.51628/001c.29674.

[28] R. Lokesh et al., "Visual accuracy dominates over haptic speed for state estimation of a partner during collaborative sensorimotor interactions," *J. Neuriophysiol.*, vol. 130, pp. 23–42, 2023.

[29] V. T. Chackochan and V. Sanguineti, "Incomplete information about the partner affects the development of collaborative strategies in joint action," *PLoS Comput. Biol.*, vol. 15, no. 12, 2019, Art. no. e1006385.

[30] M. Selvaggio, M. Cognetti, S. Nikolaidis, S. Ivaldi, and B. Siciliano, "Autonomy in physical human-robot interaction: A brief survey," *IEEE Robot. Automat. Lett.*, vol. 6, no. 4, pp. 7989–7996, Oct. 2021.